Earthquake Geotechnical Engineering for Protection and Development of Environment and Constructions – Silvestri & Moraci (Eds)
 ISBN 978-0-367-14328-2

Reconstructing mechanism of large ground movement induced by 2018 Palu Earthquake 7.4 Mw

A. Arsyad, L. Samang, T. Harianto, A.B. Muhiddin & A.R. Djamaluddin
Department of Civil Engineering, Hasanuddin University, Makassar, Indonesia

S. Aswad
Department of Geophysics, Hasanuddin University, Makassar, Indonesia

ABSTRACT: This study aims to investigate the mechanism of large ground movement occurring on typical slope model of Palu during 2018 Palu Earthquake 7.4 Mw. Typical slope model of Palu, represented by Balaroa Slope, is moderately steep, comprising of two sand layers and a silt layer located in between those sand layers. Detailed geotechnical parameters, stratigraphy, and hydrogeology of the slope model are obtained with boreholes-SPT and electrical resistivity imaging survey. A 2-dimension finite difference method of FLAC is employed to generate the slope model using Finn-Byrne liquefiable sand and typical input ground motion compatible with Palu Earthquake 7.4 Mw. The results suggested that, large magnitude of lateral ground movement is much related to the existence of low permeable silt layer separated the upper liquefiable sand and lower sand layer. Silt layer acts as an impermeable barrier between surface aquifer and confined aquifer in the slope. During the earthquake, liquefaction occurs at the near surface in the slope, and in deep ground below the slope crest. This generates such deep shear failure slip plane for driving large lateral ground movement.

1 INTRODUCTION

Earthquake 7.4 Mw has occurred in Palu, the capital city of Sulawesi Tengah Province, Indonesia at September 28, 2018. The earthquake has triggered an average 5 m height tsunami, heavily damaged around 5,000 buildings, causing at least 3,000 lives lost. The earthquake has also propagated large scale of liquefactions, resulting in lateral spreading or flow failures in several areas, including Balaroa, Petobo, Jono Oge and Sibalaya. These phenomena are so massive with deep slip failure up to maximum 15 meters, and large lateral displacements of 1 – 3 kms. The mechanism whether lateral spreading or flow failure and its contributing factors are still poorly understood, since large lateral displacement due earthquake rarely occurs in Palu, even though the city has experienced a number of large earthquakes.

Lateral spreading may be defined as displacement of gentle slope due to pore pressure building up or liquefaction in a shallow underlying deposit (Rauch, 1997). The spreading could be as fracturing extension of material (Varnes, 1978) owing to liquefaction and it is often to take place in gentle slope with 0.3% to 5% inclined ground (Bartlett aand Youd, 1992). The lateral spreading can be identified with several phenomena in slope such sand boils at the lower portion, ground fissures in the upper portion, subsidence at the head, and heaving at toe of slope. The existing ground in Palu is about 5% to 30%, so that it can be categorized as steep slope. This condition seems to be more pronounced for a flow slide, rather than lateral spreading. Flow slide is caused by dominantly contractive mechanism rather than dilative mechanism as found in lateral spreading (Ishihara, 1993). The fines content of sand layer may affect the magnitude of lateral spreading. It is about 24% - 30% of fines fractional weight to sand, causing soil to be more collapsible and liquefiable (Koester, 1994). However, for the case of 2018 Palu Earthquake, it is still difficult to determine whether lateral spreading or flow slide took place during the earthquake, and to answer the question why the ground movements occurred in such a massive scale. Therefore, this study endeavor to investigate the mechanism of the ground movement induced by liquefaction in Palu due to 2018 Palu Earthquake 7.4 Mw based on numerical simulations technique. Such numerical simulation on ground movement induced by liquefiable soil has been conducted by Seid-Karbasi and Byrne (2007) in order to examine the reason why lateral spreading and flow slides occuring for gentle slope. They utilized effective stress coupled stress-flow dynamic analyses procedure to demonstrate the effects of a low-permeability barrier layer on ground deformations from an earthquake event. Their techniques can be used for other cases such as cases in Palu.

2 2018 EARTHQUAKE AND GROUND MOVEMENT IN PALU

Palu is the capital of Sulawesi Tengah Province, Indonesia. The capital is just 76 km south of Sirenja, the epicenter of 2018 Earthquake Palu 7.4 Mw. It has been measured about 15 foreshocks with 5 Mw to 6 Mw, occurred in the city, before the main shock 7.4 Mw. The earthquakes were generated along Palu-Koro Fault with sinistral strike-slip fault mechanism. Fault offset at 2.5 m with 7 km long can be obviously seen in the city. The fault offset is a part of Palu-Koro Fault Zone, situated in the center of the Palu City from North to South with strike angle 160° NE. Geological condition of Palu is Holocene sedimentary rock, mostly sandy soil (Figure 1). Geological condition of the city is much influence by the Gawalise Mountain which is formed by plutonic rocks of granite and diorite in the west, and the Nokilalaki Mountain which has complex metamorphic rocks (Gumbasa and Wana Complex) in the east of the city. The sediment, originated from weathering the plutonic and metamorphic rocks in those mountains, forms the city. The sediment transported to, deposited and consolidated in the lowland area around the Sungai Palu, the main river of the city. Therefore, the soil can be found as fine sand, some areas with silty sand, and gravels. Previous study conducted by Irsyam (2018), has suggested that most areas in Palu is fine to moderate sand, identified as the most liquefiable soils based on Tsuchida (1970) criteria (Figure 2).

2.1 *Palu Earthquake 2018 7.4 Mw and liquefaction in Balaroa Palu*

Acceleration waveform data of Palu 2018 7.4 Mw Earthquake was obtained from JICA-BMKG, JIGS, NEC, MEISSEI, and Pacific Consultant. The data is based on the acceleration

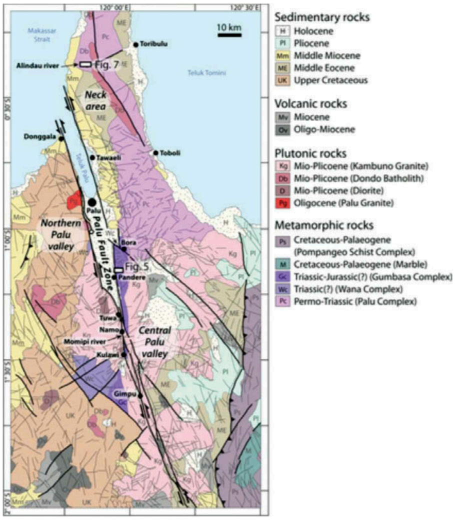

Figure 1. Geology of Palu (after Witkonson, 2011).

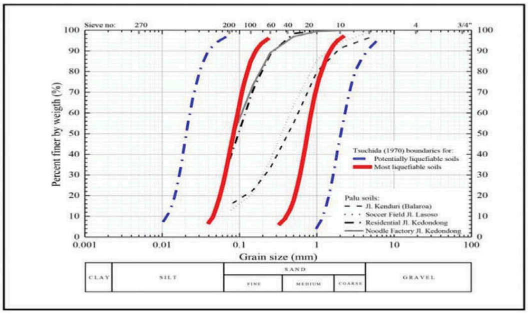

Figure 2. Grain size distribution of Sands of several areas in Palu (after Irsyam et al., 2018).

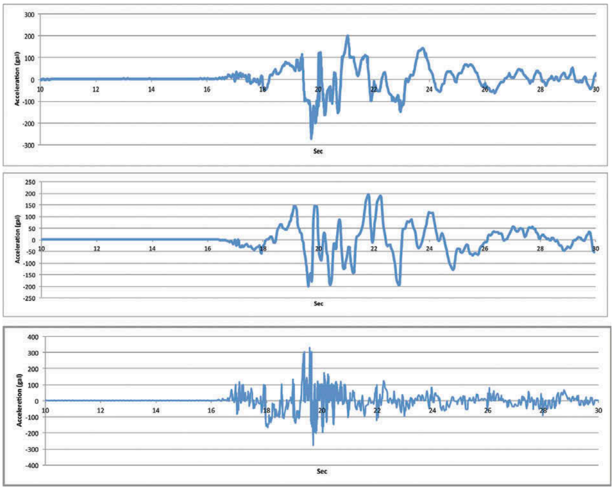

Figure 3. Accelerograms of Palu 2018 7.4 Mw Earthquake (JICA-BMKG in Irsyam, et al. 2018).

measurement of Station PCI-Palu with GPS coordinate of 0.90554S,119.83666E), located 80 km south from the epicenter of the earthquake. Figure 3 illustrates that that peak ground accelerations (PGAs) are 281 gal in EW, 203 gal in NS, and 335 gal in UD directions. It can be seen that the acceleration in vertical direction is higher than the horizontal one.

Balaroa is selected for this study as one of the area in the Palu city, experiencing a large lateral ground movement during the earthquake. This area is located at the west side of Palu, 74.24 km from the epicenter of the 2018 earthquake 7.4 Mw (Figure 4a). This area has

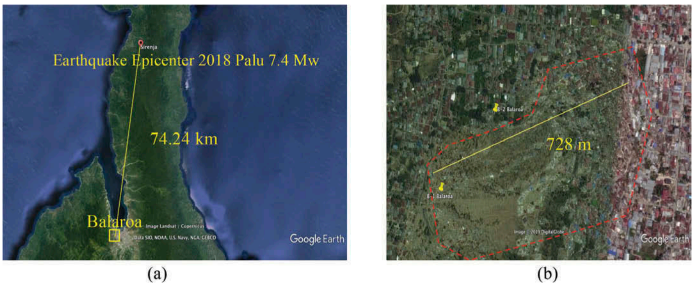

Figure 4. The location (a) and the dimension of lateral ground movement of Balaroa (Google Earth, 2019).

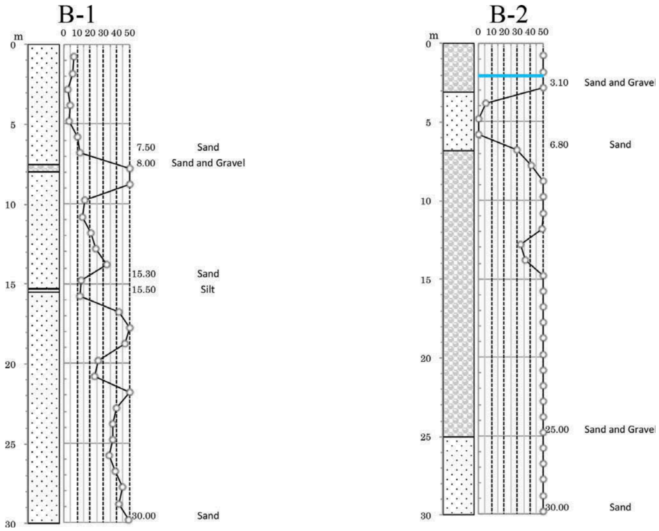

Figure 5. Borlogs of B-1 and B-2 located at Balaroa, post the earthquake 2018 7.4 Mw (after JICA team in Irsyam et al. 2018).

suffered for ground deformation during the earthquake for about 728 m (Figure 4b). Before the earthquake, Balaroa is residential area since 1980s with total area of 7.5 hectares. The area affected by ground movement induced liquefaction is almost 3 hectares. Topography of the area is a slope with 5% inclination. Figure 5 presents soil conditions of the area of Balaroa based on two boreles (B-1 and B-2) conducted after the disaster. B-1 is located inside the affected area, while B-2 is outside the affected area. It is obvious that the soil condition between those areas reveal such difference. The ground condition of the affected area (B-1) has distinctive soil layers, sand layers (8 m thick) above sand and gravels (0.5 m). Below those layers, there is a sand layer with 7 m thick underlying by silt (1 m thick). Sand layer is from the depth of 16 m to 30 m. In contrast, the unaffected area (B-2) does not have similar stratigraphy condition with B-1. The ground condition is upper sand and gravel layer (3 m thick), underlying by loose sand (3.8 m thick). From the depth of 6.8 m to 25 m, sand and gravel is found. Sand layer is at the bottom (25 m to 30 m).

2.2 *Geo-resistivity soil profiles of Balaroa*

The aquifer condition of Balaroa was investigated through geo-resistivity measurement, and the result can be seen in Figure 6. It is found that upper loose sand saturated with water at a 6.8 m thick in the slope crest up to 13.4 m thick in the slope toe. Below the upper loose sand with water, there is low permeable silt, and granite boulders. Its thickness varies from 5 to 7 m. Below that layer, saturated silty sand layer is found with about 20 m thick. Bedrock of

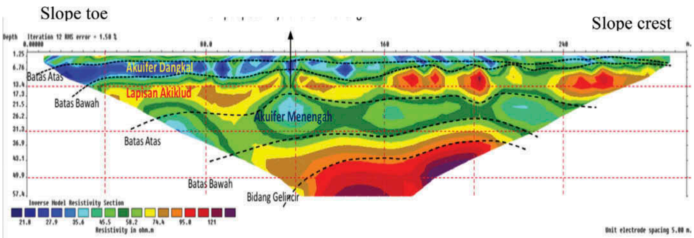

Figure 6. Geo-resistivity profiles at Balaroa after Palu Earthquake 2018 7.4 Mw.

granite is found below the silty sand. This suggested that unconfined aquifer is found at the surface before low permeable layer of silt. Such confined aquifer is found below the silt layer to granite bedrock. Since the geo-resistivity profile was conducted after the earthquake, it can be suggested that the upper loose sand layer is originally 10 m to 20 m thick. The earthquake has generated the collapsing and movement of soil with at least 15 m thick.

3 NUMERICAL SIMULATION

To investigate ground movement due to Palu Earthquake 7.4 Mw, a slope, which can model soil condition of Balaroa, was simulated using dynamic analysis and liquefaction modeling of FLAC (Itasca, 2003). In this case, the deformation of the liquefiable soil and its displacement propagated by earthquake motion was computed. The simulation was also conducted to obtain the development of excess pore pressures in the soil generating by liquefying and displacement of soil. Balaroa slope model consist of upper fine sand and lower sand layers, which can be characterized as liquefiable sand. There is a silt layer in between those layers. The slope is 10 m high with slope angle of 25°. The slope is subjected to an earthquake motion with a peak acceleration 0.346g and duration of 25 seconds. Therefore, the acceleration data of Kochaeli 1999 7.51 Mw in strong-motion database of Pacific Earthquake Engineering Research Center (PEER) was used as dynamic loading input (Figure 7). For groundwater phase of the simulation, the permeability, porosity and water bulk modulus for upper and lower sands were assumed to be 1×10^{-12} m^2/Pa.s, 0.1, 200 MPa, respectively. While, for silt layer, those parameters were set to be to be $1\times10^{-1\circ}$ m^2/Pa.s, 0.3, 200 MPa, respectively. Meanwhile, only upper sand layer was set to be potentially liquefiable in relation to standard penetration test (SPT) results. Consequently, $(N1)_{60}$ of 10 was selected for this layer to determine the parameters C1 and C2 in the Finn-Byrne liquefaction model in FLAC. For a normalized SPT blow count of 10, the Finn (1975)-Byrne (1995) model parameters are C1 = 0.245 and C2 = 0.815. Other mechanical parameters of soils were assigned through several values as seen in Table 1.

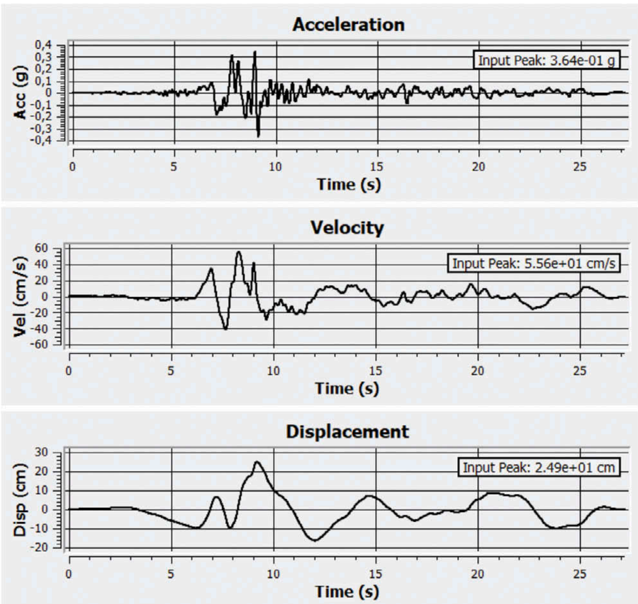

Figure 7. Input ground motions of the model.

Table 1. Drained soil parameters of Balaroa Model.

Mechanical parameters	Upper fine sand	silt	Lower silty sand
Dry Density (kg/cm3)	2000	1600	1715
Bulk Modulus (MPa)	10.0	2.67	10.0
Shear Modulus (MPa)	6.0	1.6	6.0
Cohesion (Pa)	0	2000	0
Friction angle (degrees)	40	20	25

4 RESULTS AND DISCUSSIONS

4.1 *Earthquake simulation with soil liquefied in Palu slope model*

To investigate the development of slope failure during dynamic loading, the development of shear-strain concentration bands within the shear-strain contour plots in the slope were estimated. Figure 8 displays the contour plot of shear strain increment for the slop model during the period of earthquake. The shear strain is propagated below the silt layer at the beginning of earthquake at 2 seconds. Then, shear strain increases significantly at the area near slope toe below silt layer, while it also propagates to slope crease. The soil layers where the shear failure propagated have created such a slip failure plane. As a result, the slope surface deforms and moves. The results also indicated that liquefaction is generated at the soil layer located at near surface of the slope toe, while the liquefaction only occurs at several meters below the slope crest. As the earthquake intensifies, slope moves laterally and creates heave in the slope toe and subsidence in the slope crest. The deformation of the slope model can be seen obviously in Figure 9. The silt layer deforms so badly due to increase excess pore pressure in the layer below induced by the earthquake. This may lead to such silt layer collapse, and water from the confined aquifer below the silt layer could flow out to surface aquifer, particularly at the slope toe. It must be noted that the simulation was ended

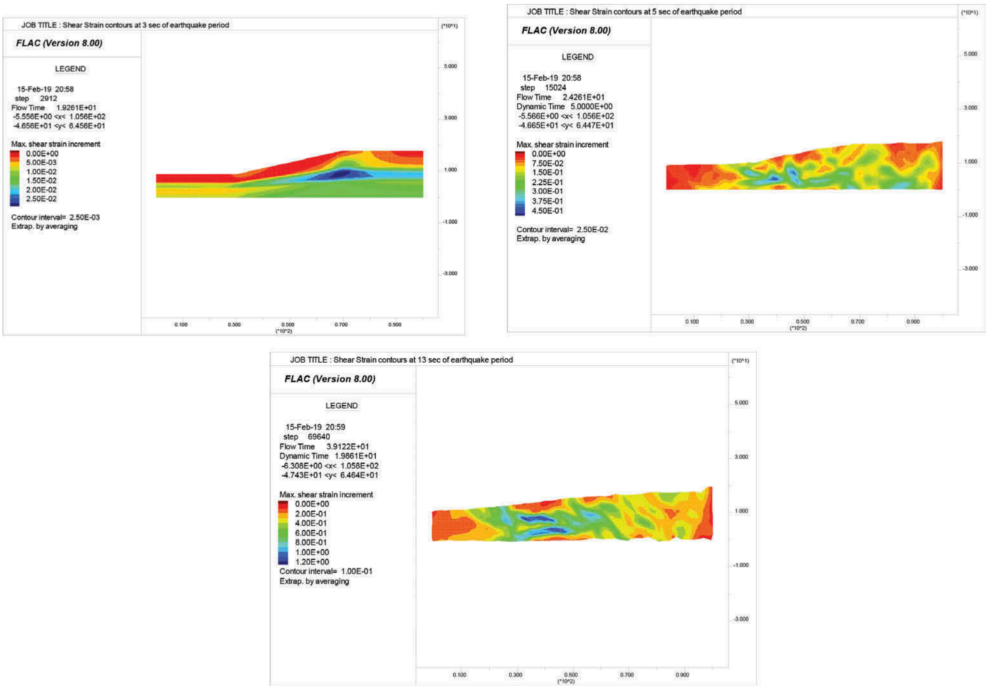

Figure 8. Shear strain contours at the period of 2, 5, and 13 seconds simulated in the slope model during earthquake.

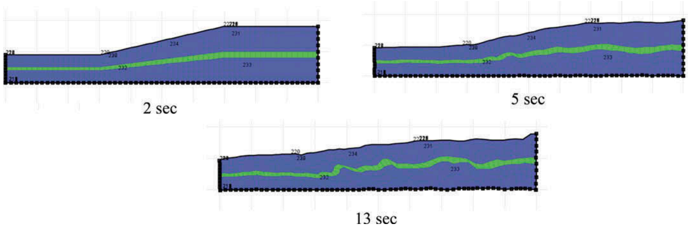

Figure 9. The deformation on the slope model during the earthquake.

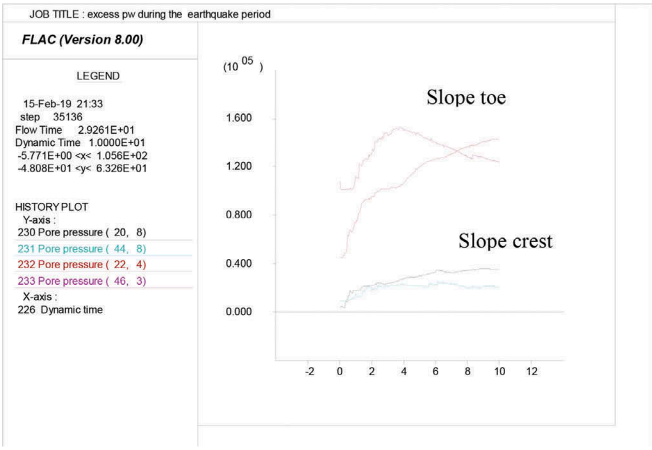

Figure 10. Excess pore pressures in the slope toe and slope crest during the earthquake.

just 13 seconds due to the large change of the model geometry. However, this corresponds to the maximum acceleration of the earthquake is already passed, at 12 seconds, and subsequently the acceleration declined since then until the last period of earthquake at 25 seconds.

4.2 *Excess pore pressures*

Earthquake excitation on the slope generates excess pore pressure. Figure 10 shows that the increase of excess pore pressure below the silt layer is larger than that in the soil near surface. During the earthquake, the excess pore pressure still builds up at the area below the slope toe, while that in the area below the slope crest has already been at the peak, for the period of earthquake at 4 seconds. As earthquake intensifies at the period 12 seconds, the excess pore pressure below the slope toe has reached the peak, whereas that below the slope crest has been declined and then stabilized. The results indicated that pore pressure at slope toe is slowly increased than that at slope crest. However, slope toe is the critical area where excess pore pressure increases dramatically following the excitation of earthquake. This is well agreement with larger shear strain occurred at slope toe that the slope crest. It means that lateral spreading starts on the deformation slope toe, followed by slope crest.

5 CONCLUSIONS

Several findings in this study can be explained as below:

– At the beginning of the earthquake, seismic loading induces the increase of pore pressure, generating shear strain just below the silt layer.

- As the earthquake is continuing and intensifying, the shear strain propagates, and breaks the silt layer, leading to the groundwater flowing out from confined to the surface aquifer, particularly at the area below the slope toe.
- Massive liquefaction occurs in the near surface of soil around the slope toe, then it moves to the ground located several meters below the slope crest. As a result, slip failure plane is created, driving the slope to move laterally. The ground in the slope crest subsides and collapses.
- Shear strain increment creates failure planes at several meters below surface, causing deep lateral displacement, and the surface becomes collapsing.
- Slope toe has become the most critical area, which is more vulnerable to generate flow slide.

ACKNOWLEDGEMENT

This work would not have been possible without technical and data support from Japan International Cooperation Agency (JICA) team for Palu Earthquake disaster, and Pacific Earthquake Engineering Research (PEER) Center, and ITASCA consulting group. We would like to extend our gratitude to Professor Mitsu Okamura of Ehime University and Professor Hemanta Hazarika of Kyushu University Japan, and Dr. Purwanto of Hasanuddin University for valuable advice and technical guidance.

REFERENCES

Bartlett, S.F., and Youd, T.L. 1992, “Empirical Analysis of Horizontal Ground Displacement Generated by Liquefaction-Induced Lateral Spread,” National Center for Earthquake Engineering Research, Technical Report NCEER-92-0021.

Byrne P.M., A Cyclic Shear-Volume Coupling and Pore-Pressure Model for Sand, in Proceedings: Second International Conference on Recent Advances in Geotechnical Earthquake Engineering and Soil Dynamics, St. Louis, 1991, Paper No. 1.24, 47-55

Finn W.D.L., Martin G.R. and Lee K.W. 1975, An Effective Stress Model for Liquefaction, Journal of the Geotechnical Engineering Division, Vol. 103, No. 6, pp. 517-533.

Ishihara, K. 1993. Liquefaction and flow failure during earthquakes. Géotechnique, 43 (3): 351-415.

Irsyam. M., 2018. Palu Earthquake 2018: Preliminary survey report. SEAGC 2018 and HATTI Conference, Jakarta Indonesia.

Itasca Consulting Group. 2003. “FLAC2D, Fast Lagrangian Analysis of Continua in 2 Dimensions, User‘s Guide”. Minneapolis, Minnesota, USA.

Koester, J.P. 1994. The Influence of Fine Type and Content on Cyclic Strength. Ground Failures under-Seismic Conditions. Geotechnical Special Publication, No. 44, 330-345.

Rauch, A. F., 1997. Empirical Method for Predicting Surface Displacements Due to Liquefaction-Induced Lateral Spreading in Earthquakes. PhD Disertation. Virginia Polytechnic and State University. USA.

Seid-Karbasi, M., Byrne, P.M., 2007, Seismic liquefaction, lateral spreading, and flow slides: a numerical investigation into void redistribution, Canadian Geotechnical Journal, 2007, 44(7): 873-890.

Tsuchida, H. 1970. “Prediction and Countermeasure against Liquefaction in Sand Deposits,” Abstract of the Seminar of the Port and Harbour Research Institute, Ministry of Transport, Yokosuka, Japan, pp. 3.1-3.33 (In Japanese).

Varnes, D., J. 1978. Slope Type Movement and Processes. TRB Special Report 176, Landslides: Analysis and Control.

Watkinson, I.M. 2011. Ductile flow in the metamorphic rocks of central Sulawesi. Geological Society, London, Special Publications, 355, 157-176, 27 June 2011.